

⁷Cunningham, F. G., "Power Input to a Small Flat Plate from a Diffusely Radiating Sphere with Application to Earth Satellites: the Spinning Plate," NASA TN D-1545, Feb. 1963.

⁸Cunningham, F. G., "Earth-Reflected Solar Radiation Incident upon an Arbitrarily Oriented Spinning Flat Plate," NASA TN D-1842, July 1963.

⁹Powers, E. I., "Thermal Radiation to a Flat Surface Rotating about an Arbitrary Axis in an Elliptical Earth Orbit: Application to Spin-Stabilized Satellites," NASA TN D-2147, April 1964.

¹⁰Bannister, T. C., "Radiation Geometry Factor between the Earth and a Satellite," NASA TN D-2750, July 1965.

¹¹Watts, R. G., "Radiant Heat Transfer to Earth Satellites," Transactions of the ASME, *Journal of Heat Transfer*, Vol. 87, Aug. 1965, pp. 369-373.

¹²Skladany, J. T., and Rochkind, A. B., "Determination of Net Thermal Energy Incident on a Satellite," ASME Paper 67-HT-56, Seattle, WA, Aug. 1967.

¹³Doenecke, J., "Thermal Radiations Absorbed by a Partially Obscured Spacecraft," *Astronautica Acta*, Vol. 15, Dec. 1969, pp. 107-117.

¹⁴Finch, H. L., Sommerville, D., Vogt, R., and Bland, D., "A Computer Program for Calculating External Thermal Radiation Heat Loads and Temperatures of Spacecraft Orbiting the Planets or the Moon," NASA TR R-278, Dec. 1968.

¹⁵Turner, R. C., "NEVADA Software Package User's Manual," 7th ed., Turner Associates, Brea, CA, Jan. 1980.

¹⁶Jensen, C. L., and Goble, R. G., "TRASYS II User's Manual," Martin Marietta, MCR-73-105 (NAS9-15832), Rev. 5, Denver, CO, June 1983.

¹⁷Prenger, Jr., F. C., and Patterson, W. C., "Earth Albedo as Determined from Skylab Data," *Journal of Spacecraft and Rockets*, Vol. 13, April 1976, pp. 244-247.

Laminar Forced Convection in Circular Duct Inserted with a Longitudinal Rectangular Plate

Jun-Dar Chen* and Shou-Shing Hsieh†

National Sun Yat-Sen University, Kaohsiung, Taiwan, Republic of China

I. Introduction

LAMINAR forced convection in circular duct with a longitudinal arbitrary-shaped inner core is encountered in a wide variety of engineering situations, such as a double-pipe heat exchanger, gas-cooled electrical cables, and a tube with removable insert as a heat transfer augmentative device in a tubular recuperator. Excellent surveys of laminar forced convections in circular and noncircular annular ducts have been presented by Shah and London¹ and Shah and Bhatti.² It was found from these surveys that, while the laminar forced convection in circular annulus had been thoroughly studied, it was apparent that very little was known about that in noncircular annulus. The regular polygon had been extensively considered as the shape of the inner core in studies of noncircular annulus.^{1,2} As one of the tubeside augmentative devices, the rectangular shaped inner core is frequently used in practical tubular recuperators. However, it has received very little attention except with the unity aspect ratio, i.e., square shape.

The point-matching method and the least squares approximation method has been applied to analyze the laminar forced convection in a circular duct with a concentric square core under the thermal boundary conditions of axially uniform heat flux and peripherally uniform temperature on the walls.^{1,2} Recently, Solanki et al.³⁻⁶ studied similar problems in which thermal boundary conditions of axially and peripherally uniform heat flux at the inner wall and insulated outer wall with peripherally constant temperature were used. The Galerkin finite element method was adopted in their numerical studies, which provided the flow³ and temperature⁴ patterns inside the noncircular annulus. However, only the flowfield was investigated in their experimental works.^{5,6} By a square core of radius ratio 0.6783, an experimental assessment for numerical result of the fRe factor was made.⁶ Excellent agreement substantiated the reliability of the numerical results. Despite the foregoing discussion, it seems that no results of a circular duct with an eccentric noncircular inner core are available in the open literature.

This paper presents a numerical study for thermally developed laminar forced convection in a heated circular duct inserted concentrically or vertically eccentrically with a longitudinal rectangular adiabatic plate. The flow passage is schematically depicted in Fig. 1 where relative geometric quantities are also shown. In addition to the flow and temperature patterns, effects of aspect ratio of insert (L/H), radius ratio of the circumscribed circle of insert to duct (RR), and vertically eccentric installation of the insert, on the laminar forced convection are determined.

II. Theoretical Analysis

Consider steady, laminar fully developed flow with constant fluid properties in the noncircular annulus of Fig. 1 in which the duct is assumed to be of axially uniform heat flux, q''_{in} , with peripherally constant wall temperature. The mathematical formulation and solution procedure are outlined in great detail by Chen and Hsieh⁷ and only a brief description is presented here. The constant axial temperature rising rate is related to q''_{in} via overall heat balance. The radius of duct, R_o , $(-dp/dz)R_o^2/\mu$ and $q''_{in}R_o/k$ are used to scale length, velocity, and relative temperature (with respect to the constant as $EV = (e_v/R_o)/(1 - RR)$). Here dp/dz = axial pressure gradient, μ = fluid dynamic viscosity, k = fluid thermal conductivity, and e_v = vertical eccentricity. Under the above assumptions, the dimensionless axial momentum and energy conservation equations are formulated as

$$\frac{\partial^2 W}{\partial X^2} + \frac{\partial^2 W}{\partial Y^2} + 1 = 0 \quad (1)$$

$$\frac{\partial^2 T}{\partial X^2} + \frac{\partial^2 T}{\partial Y^2} - \frac{WP_o}{M_m A_f} = 0 \quad (2)$$

where P_o and A_f are dimensionless outer wall perimeter and flow area and W_m is dimensionless mean velocity of the pas-

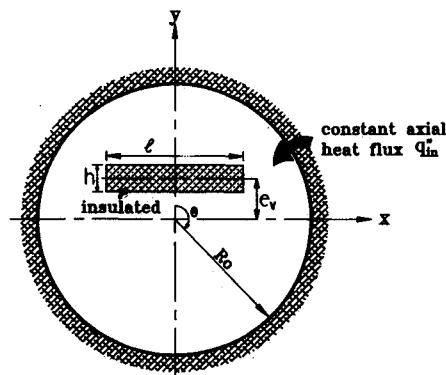


Fig. 1 Noncircular annular duct.

Received Aug. 31, 1990; revision received Dec. 10, 1990; accepted for publication Dec. 17, 1990. Copyright © 1991 by the American Institute of Aeronautics and Astronautics, Inc. All rights reserved.

*Graduate Student, Department of Mechanical Engineering.

†Professor and Chairman, Department of Mechanical Engineering. Member AIAA.

sage. The dimensionless boundary conditions are expressed as

$$W = 0; \quad \frac{\partial T}{\partial N} = 0 \quad \text{at inner wall} \quad (3a)$$

$$W = 0; \quad T = 0 \quad \text{at outer wall} \quad (3b)$$

The boundary-fitted coordinate system (BFCS) is employed to tackle the irregularity of flow passage and a 73×36 non-orthogonal boundary-fitted grid in physical domain is numerically generated with nodes equi-spaced along, and more grid lines closely packed near, both walls. Equations 1–3 are therefore transformed to the BFCS and solved by the finite volume discretized method with SLOR solver in the transformed domain. The friction factor-Reynolds number product, fRe , local and averaged outer-wall Nusselt number, Nu and Nu_m , are obtained as follows⁷:

$$fRe = D_h^2/(2W_m); \quad Nu = \left(\frac{\partial T}{\partial N}\right)_s D_h/T_b$$

$$Nu_m = -D_h/T_b \quad (4)$$

where D_h and T_b are the dimensionless hydraulic diameter and bulk temperature.

III. Results and Discussion

Present solution procedure has been validated by Chen and Hsieh⁷ with results of maximum deviation of the order of 1%. The numerical results are presented over EV value ranging from 0.0 to 0.4 for plate inserts of aspect ratios of 1, 2, 5, and 8 with RR value varying from 0.2 to 0.8. Figure 2 displays the cross-sectional contours of isotherms and normalized isovels, W/W_m , of some cases. Due to the nature of symmetry, the isovels and isotherms are plotted separately in the right and left halves of annuli with the dots denoting the positions of $(W/W_m)_{\max}$. The corresponding T_{\min} and $(W/W_m)_{\max}$ values of these cases are also listed. The contours are equi-spaced with spacing values listed below the figure. Note that the radial distribution of W/W_m value at each angular location is

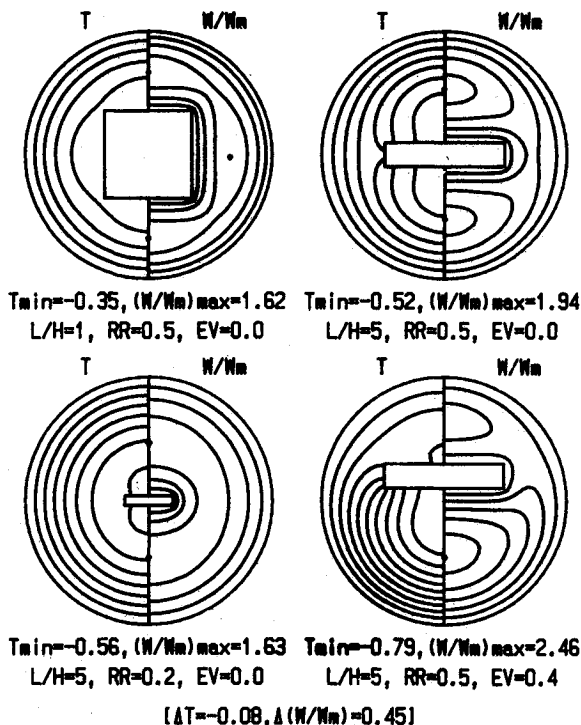


Fig. 2 Flow and temperature patterns of some cases.

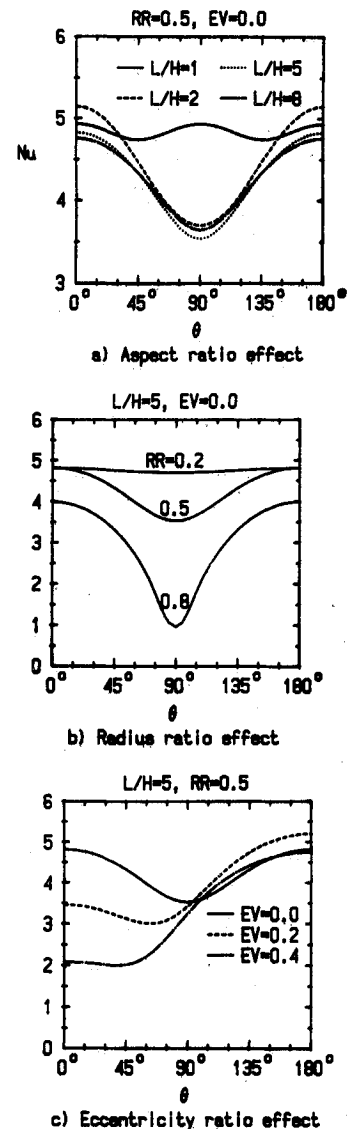


Fig. 3 Angular variations of Nu value.

nearly parabolic with a peak somewhat near the insert.³ The highest fluid temperature appears at the outer wall due to the specified heat condition. A close examination of Fig. 2 reveals that distributions of flow and inner wall temperatures are inversely proportional to that of flow rate in each annulus.

By comparing the flow and temperature patterns of the square insert ($L/H = 1$) with those of the thin-plate insert ($L/H = 5$), it is found that, under the same RR value, these patterns alter significantly as the insert shape changes from square to rectangle. Although not shown, similar patterns to those of thin-plate insert are also observed for plate inserts of $L/H = 2$ and 8. Symmetry about the diagonal of the insert is found in the square insert case. For each insert, it is found from the isovel distribution that the aforementioned W/W_m peak is highest at angular location through the center of the gap having the largest clearance and lowest through that having the smallest clearance. This implies that the flow rate through a gap is proportional to its clearance. The isotherms are circular near the outer wall and deflect toward the insert due to its adiabatic condition.

Two thin-plate inserts of $RR = 0.2$ and 0.5 are chosen to investigate the effect of radius ratio on the flow and temperature patterns. At $RR = 0.2$, the radial distribution of axial velocity shows little angular variation and the isotherms are circular in most regions. As the RR value increases, however, the flow rate increases, but fluid temperature decreases in the high flow rate region. The opposite trend occurs in the low

flow rate region. As a result, the flow and temperature patterns become more angularly variant.

The effect of vertically eccentric installation of the insert on flow and temperature patterns is typically presented by placing the concentric ($EV = 0.0$) thin-plate insert of $RR = 0.5$ in a vertically eccentric position ($EV = 0.4$). Upwardly shifting the insert increases and decreases, respectively, the flow rates in the lower and upper regions and causes the angular location of the lowest W/W_m peak to shift from the location in the concentric case to the upper region. Consequently, higher and more uniform fluid temperatures exist in the upper region.

A. Local Nusselt Number

Angular variations of local Nusselt number, Nu , of representing cases are displayed in Fig. 3 in which the angular coordinate, θ , is measured clockwise from the positive y axis (Fig. 1). Due to the nature of the symmetry of temperature pattern, such variations are presented over θ values ranging from 0 deg (through the upper gap center) to 180 deg (through the lower gap center). Comparison with the flow pattern shows that the distribution of Nu value is proportional to that of flow rate in each annulus.

The angular variations of the Nu value of various aspect ratio inserts with $RR = 0.5$ are depicted in Fig. 3a. In accordance with the flow pattern of each insert, wavy variation for the square insert and sinusoidal-like variations for other plate inserts are observed. The difference between the highest and lowest Nu values becomes significant in cases of rectangular plate inserts. As evidenced in Fig. 3b by thin-plate insert with various RR values, the angular variation of Nu value is nearly negligible for $RR = 0.2$ and becomes more appreciable with increasing the difference between the highest and lowest Nu values as the RR value increases. The reason for the increase of difference is attributed to the increase of fluid temperature in the low flow rate region with the increase of RR value. The higher the RR value is, the larger the difference becomes. Figure 3c shows the angular variations of Nu value of the thin-plate insert with $RR = 0.5$ for various EV values. It is found that eccentrically placing the insert vertically decreases the lowest Nu value and the θ value where it occurs. The difference between the highest and lowest Nu values increases with the increase of EV value.

B. Overall Friction Factor and Nusselt Number

Tables 1 and 2 summarize the fRe factors and Nu_m values of some inserts with concentric installation and vertically ec-

centric installation, respectively. A close examination of Table 1 reveals that the fRe factor and Nu_m value of the square insert are less sensitive to the RR value than those of any other plate insert. For the square insert, the fRe factor increases first then reaches a maximum at a certain RR value with the increase of the RR value.¹ It is also the case for the Nu_m value. For any other plate insert, while the fRe versus RR relations are similar to that of the square insert, the Nu_m value decreases with the increase of the RR value. Note that the higher the aspect ratio of insert is, the lower the RR value of the largest fRe factor becomes. Note that the fRe factor and Nu_m value of inserts with large aspect ratios ($L/H \geq 5$) are nearly independent of the aspect ratio. Generally speaking, in these studied installations, the square insert has the highest fRe factor and Nu_m value for each RR value among the inserts studied.

The effect of vertically eccentric installation of inserts of $RR = 0.5$ with various aspect ratios on the fRe factor and Nu_m value is given in Table 2. In the $L/H = 5$ case, results of $RR = 0.2$ and 0.8 are also provided for reference. For each insert, the vertically eccentric installation is found to decrease the fRe factor and Nu_m value. The higher the aspect ratio of insert is, the slower the decreasing rate becomes. Note that the fRe factor and Nu_m value of plate insert of $L/H \geq 5$ are also nearly independent of the aspect ratio in the vertically eccentric installation case.

IV. Conclusions

The thermally developed laminar forced convection in an axially uniformly heated circular duct inserted concentrically or vertically eccentrically with an adiabatic longitudinal rectangular plate has been numerically studied. The flow rate through a gap is found proportional to the gap clearance. The distribution of the local Nusselt number is proportional, but those of fluid and inner wall temperatures are inversely proportional to that of flow rate in each annulus. Inserts of rectangular cross section have similar flow and temperature patterns that are different from those of the square insert. The square insert has been shown to have the highest fRe factor and Nu_m value at each RR value studied. Vertically eccentric installation of the insert decreases the fRe factor and Nu_m value. The higher the L/H value, the slower the decreasing rate. The fRe factor and Nu_m value of the insert of large aspect ratio become nearly independent of the aspect ratio in concentric and vertically eccentric installations.

References

- ¹Shah, R. K., and London, A. L., *Laminar Flow Forced Convection in Ducts*, 1st ed., Academic Press, New York, 1978.
- ²Shah, R. K., and Bhatti, M. S., "Laminar Convection Heat Transfer in Ducts," in *Handbook of Single-Phase Convection Heat Transfer*, 1st ed., edited by S. Kakac, R. K. Shah, and W. Aung, Wiley, New York, 1987, Chap. 3.
- ³Solanki, S. C., Saini, J. S., and Gupta, C. P., "Flow Through in Doubly Connected Ducts," *International Journal of Heat and Fluid Flow*, Vol. 7, 1986, pp. 301-306.
- ⁴Solanki, S. C., Prakash, S., Saini, J. S., and Gupta, C. P., "Forced Convection Heat Transfer in Doubly Connected Ducts," *International Journal of Heat and Fluid Flow*, Vol. 8, 1987, pp. 107-110.
- ⁵Solanki, S. C., Krishna Murthy, M. V., and Ramachandran, A., "Flow Through Non-Circular Passage," Joint ASME/CSME Fluid Engineering Conference, Paper 70-FE-12, Niagara Falls, NY, 1979.
- ⁶Solanki, S. C., Saini, J. S., and Gupta, C. P., "An Experimental Investigation of Fully Developed Laminar Flow in a Non-Circular Annulus," 8th National Conference on Heat and Mass Transfer, HMT-A34-85, Visakhapatnam, 1985.
- ⁷Chen, J. D., and Hsieh, S. S., "Assessment Study of Longitudinal Rectangular Plate Inserts as Tubeside Heat Transfer Augmentative Devices," *International Journal of Heat and Mass Transfer*, in press.

Table 1 fRe factor and Nu_m value in a concentric case

L/H	fRe/Nu_m for RR			
	0.2	0.4	0.6	0.8
1	22.50/4.818	23.03/4.852	23.09/4.806	21.68/4.237
2	22.41/4.799	22.68/4.691	21.48/3.994	17.24/2.620
5	22.15/4.762	22.23/4.552	20.46/3.863	16.54/2.993
8	22.02/4.748	22.12/4.536	20.49/3.932	17.04/3.213

Table 2 fRe factor and Nu_m value in an eccentric case

L/H	RR	fRe/Nu_m for EV		
		0.0	0.2	0.4
1	0.5	23.15/4.853	22.28/4.331	20.06/3.453
2	0.5	22.34/4.456	21.54/3.946	19.47/3.118
5	0.2	22.15/4.762	21.41/4.482	19.51/3.971
	0.5	21.63/4.269	21.03/3.923	19.44/3.281
	0.8	16.54/2.993	16.43/2.927	16.10/2.755
	0.5	21.55/4.279	21.01/3.976	19.56/3.387